RSC Advances

ROYAL SOCIETY
OF CHEMISTRY

www.rsc.org/advances

RSC Advances

Dynamic Article Links ▶

COMMUNICATION

Controllable synthesis of obvious core-shell structured Y/Beta composite zeolite through a stepwise-induced method

Bo Ren, Shiyang Bai, Jihong Sun*, Faqian Zhang and Minghui Fan

A stepwise-induced method is firstly proposed with *easy and simply preparations*, by which the *obvious core-shell structured Y/Beta composite zeolite* was successfully prepared using pre-synthesized NaY-zeolite as starting materials. The composite
10 **zeolites with adjustable BEA/FAU features preliminary present a good catalytic performance for cumene cracking, showing a strong potential application in petroleum processing.**

Zeolites are a family of crystalline microporous aluminosilicate 15 materials, which are widely used as catalysts in petrochemical industry, due to the presence of strong acid sites and shape-selectivity induced by molecular-sized microporosity.[1-4] Among the zeolites used on an industrial scale today, zeolite Y with three-dimensional pore structures and inherent surface acidity is a 20 highly versatile used in the petroleum chemical industry field presently.[5,6] Similarly, significant attentions have been forced on zeolite Beta, which is a high-silica microporous zeolite and also possesses an interconnected three-dimensional pore network with an approximate diameter of 0.75-0.80 nm and 1.20-1.30 nm at the 25 intersections.[7-9]

In the past decades, great efforts have been made to improve the gasoline quality and increase light oil yield in the oil refining and petrochemical industries. For this purpose, several researches have been conducted on the subject of mixing of different zeolites 30 or adding some additives to zeolites as the FCC (Fluid Catalytic Cracking) catalysts,[10-13] achieving novel catalysts with extraordinary catalytic performance as compared to the single zeolites. Although the mechanically mixed zeolites have little synergistic effect and hard to homogeneously mix in micro- or 35 nano-scale level. On the basis of these fact the principle aim of the present paper is to highlight the major successes on synthesis of a novel composite zeolite with a hierarchical structure, such as MFI/MOR,[14,15] MFI/BEA,[16,17] FAU/LTA,[18] FAU/EMT,[19] FAU/BEA,[20-22] describing the benefits of their adjustable acidity, 40 adsorption/separation and hydrophilic/hydrophobic properties. In this respect, various routes for the synthesis of micro/mesoporous composite materials have been initially explored,[23-26] but the poor hydrothermal stability of mesoporous structures in composite materials has not yet been resolved, directly leading to the much 45 limitation on their extensive applications. Recently, the core-shell structured composite zeolites with two types of zeolites have been prepared, and the preliminary investigations presented enhancement in the synergistic effects in between and therefore reduction in the non-shape-selectivity occurrences. Bouizi et al.[17] 50 proposed a pre-seeding (core)-deposited nanoseed (shell) method to synthesize the core-shell structured composite zeolites (BEA/MFI), which is very common and can be employed to synthesize various kinds of composite zeolites.[14,18,19] But, the resultant particles of the prepared samples were too large to use 55 in the field of catalysis, meanwhile, the synthesis pathways were rather complicated, including the modification of positive surface charge of the large core crystal (BEA-type) by using poly(diallyldimethylammonium) as polycation agent, and overgrowth of the negatively charged nanoseeds (MFI-type) via a 60 hydrothermal treatment. Li et al.[21] prepared a novel Y/Beta composite zeolite using NaY zeolite powder as a core as well as the nutrients for Beta zeolite growth. As compared with Bouizi et al. proposed method,[17] this synthesis procedure was obviously simple without surface treatment and seed absorbing on the core 65 surface of crystal particles. Meanwhile, the obtained composite zeolite Y/Beta exhibited higher catalytic activity and selectivity than a physical mixture of Beta and Y zeolites. However, it is very noticeable that the feature of core-shell structures was unobvious on the basis of SEM and TEM images,[20-22] although 70 the XRD of this composite clearly revealed the presence of characteristic peaks of zeolites Beta and Y. Besides that, Li et al.[27] also used TEA$^+$-exchanged NaY zeolite powder as a core and then added into the pre-crystallized mixture for producing zeolite Beta, the resulting structure of the as-synthesized samples 75 presented more obvious core-shell zeolite composite, but the NaY zeolite powder needed to be ion-exchanged twice in the solution (0.5 M TEA$^+$), and it was also observed that the whole synthesis procedure was more complex than the surface treatment method.[17-19] In this study, attention was paid to the stepwise-80 induced synthesis strategy to prepare a Y/Beta composite zeolite with obviously core-shell structured characteristics in extremely dense system. Which proved to be one of the convenient, facile and effective method without filtration of pre-synthesized zeolite Y and surface treatment of zeolite particles as compared to the 85 reported methods.[16-19, 21]

The sol-gel of core-Y zeolite containing the presynthesized NaY-zeolite was firstly carried out, and then, the aqueous solution of TEAOH (35%) was added. The third step involves the addition of silica (particle size was about 50 nm) and a certain 90 amount of sulfuric acid to form new mixture with a molar composition of the gel : Na$_2$O : Al$_2$O$_3$: SiO$_2$: TEAOH : H$_2$O : H$_2$SO$_4$ = 4.7 : 1 : 15 : 3.9 : 260 : 4.7. Finally, the solid products

were obtained via hydrothermal treatment. The detailed synthesis was described in ESI section.
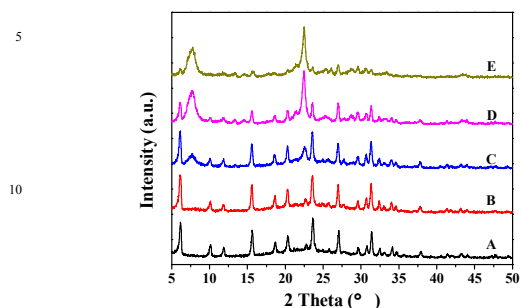
Results and discussion

Fig. 1 XRD patterns of the Y/Beta composite zeolites with a crystallization time (A) 0 h; (B) 68 h; (C) 70 h; (D) 74 h; (E) 84 h.

Fig. 1 shows the XRD patterns of the as-synthesized Y/Beta composite zeolite with different second-step crystallization time. As the previous report,[20] the relative amounts of zeolite Y and zeolite Beta contained in the Y/Beta composite zeolite were estimated by comparing the area of the selected diffraction peaks of (111), (331), (642), (555) for zeolite Y and that of (101), (300), (302) for zeolite Beta according to relationship between the weight percent of zeolite Y and corresponding peak-areas amount of zeolite Y in the mixture of zeolite Y and Beta (ESI). As can be seen, when the crystallization time was less than 70 h, Fig. 1A and B obviously present the typical characteristic diffraction peaks of zeolite Y phase. Notably, Fig. 1C appears the zeolite Beta phase when the crystallization time reached up to 70 h, however no pronounced change was found in the intensity of diffraction peaks of the zeolite Y. After that, the relative amount of zeolite Beta in the composite zeolite Y/Beta gradually increased with the prolonged crystallization time, for instance, as depicted in Fig. 1C and D, the enhancement in mass fraction of zeolite Beta phase in the Y/Beta sample was from 25 % to 70 %, more than that of zeolite Y in the resultant composite zeolite when the crystallization time was increased to 74 h. Finally, Fig. 1E displays that the crystalline phase of the composite zeolite Y/Beta was completely transformed into that of the pure zeolite Beta as the crystallization time was around 84 h. Apparently, the mass fraction between zeolite Y and zeolite Beta in the composite zeolite could be comparably adjusted via controlling crystallization time, and therefore it could be concluded that Y/Beta composite zeolite just exists in the form of intermediate state. These observations clearly demonstrate the supernate rather than solid Y zeolite particles of the pre-synthesized zeolite Y took part in the actual reaction at first and then gradually formed a little amount of zeolite Beta, which wrapped the surfaces of zeolite Y particles. These wrapping structures with core-shell characteristics could be further proved by SEM and TEM images in the following description. Therefore, this synthesis procedure is named as stepwise-induced method.

Meanwhile, the size and morphology of the pre-synthesized zeolite Y particles as well as the growth behaviors of the composite zeolite were also investigated using SEM (Fig. 2) and TEM (Fig. 3) observations. As seen, Fig. 2A reveals the spherical crystals with a fine particle size of 0.8-1.0 μm, which can be attributed to pure phase of zeolite Y particles, in good agreement with the demonstration of XRD pattern in Fig. 1A. When the crystallization time was extended to 68 h, Fig. 2B shows that the surfaces of zeolite Y were wrapped with silica nanoparticles (around 50 nm as insert imaged in Fig. 2B), which was added in the second-step. Moreover, as the crystallization time was further increased to 74 h, there were two phases appeared in the distinct micrograph of the composite zeolite Y/Beta, as shown in Fig. 2C. Specifically, the irregularly spherical phase with a much more coarse surface was attributed to the defective composite zeolite Y/Beta with particle size of around 1.5~2.0 μm. As further magnified, Fig. 2D presents a whole particle of composite zeolite Y/Beta in size of about 2.0 μm, whose surface was composed of many truncated octahedral nanoparticles with the size of around 500 nm, which was assigned to the typical morphology for zeolite Beta.[1, 9]
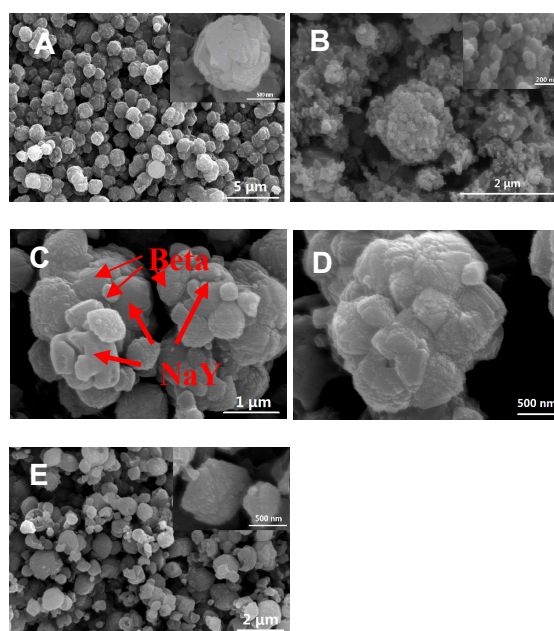

Fig. 2 SEM images of the pre-synthesized Y-zeolite (A) and Y/Beta composite zeolite with a crystallization time, (B) 68 h; (C) and (D) 74 h; (E) 84 h.

In addition, the presence of a little quantity of the mono dispersed particles was noticed (Fig. 2C), the basic reason for this was due to constant growing via the stepwise-induced method, leading to occurrence of the deciduous shell (zeolite Beta) from composite zeolite surface. When the crystallization time was prolonged to 84 h, the monodispersed particles of zeolite Beta with a diameter size of 0.5-1.0 μm were observed in Fig. 2E, however, the characteristic peaks of zeolite Y in XRD patterns were almost vanished. Therefore, the absence of zeolite Y evidently supported the stepwise-induced mechanism and is in good agreement with the results of XRD patterns in Fig. 1E.

For more detailed information, as the crystallization time was 70 h, TEM image presents the phase of zeolite Beta on the particle surface of the zeolite Y (Fig. 3A), which is in consistence with the observations of XRD pattern in Fig. 1C. The TEM

images of Y/Beta composite zeolite (Fig. 3B) reveal the obvious core-shell structures. Particularly, the magnified image (Fig. 3C) illustrates the well-ordered micropore channel array of the particle surface, indicating a highly crystallized microstructure. Furthermore, the chemical composition of a given zeolite is an important characteristic, which can define its type. As can be seen in Fig. 3D, taken sample (crystallization time is 74 h) as an example, the selected particle presents defective core-shell structure, but partly without the shell of Beta phase, which is very conductive to EDX analysis. In this regard, EDX analysis indicates that Si/Al ratio of uncovered core and bared shell was around 2.52 (Area a) and 8.54 (Area b), which were ascribed to Y phase and Beta phase, respectively. Particularly, Area c contained both zeolite Y and Beta, and its Si/Al ratio was about 6.07. Evidently, the demonstrations of EDX characterization provide us a strong and direct evidence to prove the core-shell structure of Y/Beta composite zeolite. As compared with previous studies, the SEM and TEM images revealed that composite zeolite Y/Beta had prominent features of a core-shell structure, which is more obvious than that of the Li et al. studies.[17-19]
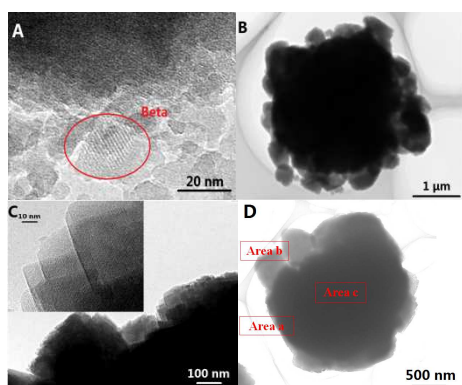

Fig. 3 TEM images of Y/Beta composite zeolite with a crystallization time, (A) 70 h; (B); (C) 74 h and magnification (insert), (D) for EDX analysis.

The thermogravimetric analysis and corresponding weight loss percent as a function of temperature of all samples were collected in Tab. 1. In general, at below 250 ^{o}C, the weight loss was mainly ascribed to the removal of adsorbed water (on the particles surface and in the micropores). In the present study, the zeolite Y was synthesized from inorganic aluminosilicate gel systems, therefore there was a certain amount of adsorbed water (but no organic template) in the micropores. Whereas, the micropores in the zeolite Beta were filled with structure directing agent (organic template) before calcined, and therefore its weight loss was attributed to the adsorbed water existing on the surface of particles. In this regard, the weight loss of zeolite Y was obviously more than that of zeolite Beta during the periods of the temperature below 250 ^{o}C. On the other hand, in the temperature span from 250 to 550 ^{o}C, the loss of mass was mainly connected with the decomposition of the structure directing agent existing in the micropores, so the higher weight loss was observed in zeolite Beta. Hence, according to the above discussion, the thermogravimetric analysis could be used to judge the presence of approximate relative content of water in the composite zeolite. As summarized in Tab. 1, with the elongated crystallization time, the weight loss of all samples below 250 ^{o}C was reduced from 11.32 % to 5.71 %, but increased from 6.73 % to 12.44 % in a temperature range of 250-550 ^{o}C. These observations clearly

indicated the decreasing of relative content of zeolite Y, but the increasing of the content of zeolite Beta with the prolonged crystallization time, which is in good agreement with the illustrations obtained form XRD patterns (Fig. 1).

Tab. 1 Summaries for weight loss as a function of temperature by thermogravimetric data obtained in N_2 atmosphere.

Sample (Crystallization time, h)	Signal (Temperature, ^{o}C)		
	< 250 ^{o}C (wt %)	250-550 ^{o}C (wt %)	>550 ^{o}C (wt %)
68	11.32	6.73	1.84
70	9.17	8.74	1.26
74	7.36	11.35	1.85
84	5.71	12.44	1.29

Evidently, the thermal stability of zeolite is an important parameter for their application in various fields.[29] Taken sample (crystallization time is 74 h) as an example, both XRD pattern and DSC profile were employed to investigate its thermal stability of the core-shell structures. The observations that its unchanged diffractive intensity of the characteristic peaks calcined at 850 ^{o}C in XRD pattern and no obvious phase transition exothermic peak at below 1000 ^{o}C in DSC curve clearly indicate the high thermal stability. The detailed illustrations were listed in the ESI section.

In addition, the cracking activities were preliminary evaluated with cumene as a probe molecule (ESI). For instance, the catalytic performance of the composite zeolite at crystallization time of 74 h presented that the conversion of cumene reached as high as 86 % at 300 ^{o}C for at least 400 min, showing that the composite zeolite had an excellent catalytic properties for cracking reaction and anti-carbon deposition ability.

Conclusions

In summary, a bi-phase BEA/FAU-type composite zeolite with obvious core-shell structure was synthesized, and the relative amount of zeolite Y or zeolite Beta in the composite zeolite could be adjusted via controlling crystallization time. Furthermore, the possible formation mechanism of Y/Beta composite zeolite was proposed as the over growing a layer of zeolite Beta around the core of zeolite Y. *A stepwise-induced method* is therefore proposed to own many advantages such as easy handling, simple procedure and controllable crystallization. Particularly, the tedious filtration and the surface treatment for pre-synthesized zeolite Y were unnecessary during the whole synthetic pathway, as compared with current preparations.[12-20, 25] The resulting BEA/FAU-type composite zeolite may has a strong potential application in petroleum processing due to its hierarchical structure, which is useful for diffusive modification of reactant molecules and in appropriate adjustment for acidic gradient distribution.

Acknowledgements

Notes and references

Beijing University of Technology, Beijing, China. Fax: +86 10-67391983; Tel: +86 10-67396118; E-mail: jhsun@bjut.edu.cn

1 C. Kanghee, N. Kyungsu, K. Jaeheon, T. Osamu and R. Ryong. *Chem. Mater.*, 2012, 24, 2733.
2 F. J. Liu, T. Willhammar, L. Wang, L. F. Zhu, Q. Sun, X. J. Meng, W. Carrillo-Cabrera, X. D. Zou and F. S. Xiao. *J. Am. Chem. Soc.*,2012, 134, 4557.
3 I. Fechete, P. Caullet, E. Dumitriua, V. Huleac and H. Kessler. *Appl. Catal. A*, 2005, 280, 245.
4 V. Mavrodinova, M. Popova, R. M. Mihályi, G. Pál-Borbély and Ch. Minchev. *Appl. Catal. A*, 2003, 248, 197.
5 D. W. Breck and N. Y. Tonawanda. US, Patent, 3130007, 1964.
6 D. Karami and S. Rohani. *Ind. Eng. Chem. Res.*,2009, 48, 4837.
7 R. L. Wadlinger, G. T. Kerr and E. J. Rosinski. US, Patent, 3308069, 1967.
8 K. Möller, B. Yilmaz, R. M. Jacubinas, U. Müller, and T. Bein. *J. Am. Chem. Soc.*, 2011, 133, 5284.
9 F. Taborda, T. Willhammar, Z. Y. Wang, C. Montes and X.-D. Zou. *Microporous Mesoporous Mater.*, 2011, 143, 196.
10 I. P. Dzikh, J. M. Lopesa, F. Lemosa and F. R. Ribeiroa. *Appl. Catal. A*, 1999, 176 , 239.
11 J. S. Buchanan and Y. G. Adewuyi. Appl. Catal. A, 1996, 134, 247.
12 F. N. Guerzoni, J. Abbot. *Appl. Catal. A*, 1994, 120, 55.
13 F. N. Guerzoni and J. Abbot. *J. Catal.*, 1993, 139, 289.
14 Y. Bouizi, L. Rouleau, V. P. Valtchev. *Microporous Mesoporous Mater.*, 2006, 91, 70.
15 J. J. Zheng, X. W. Zhang, Y. Zhang, J. H. Ma and R. F. Li. *Microporous Mesoporous Mater.*, 2009, 122, 264.
16 N. Lauridant, T. J. Daou, G. Arnold, J. Patarin and D. Faye. *Microporous Mesoporous Mater.*, 2013, 166, 79.
17 Y. Bouizi, I. Diaz, L. Rouleau and V. P. Valtchev. *Adv. Funct. Mater.*, 2005, 15, 1955.
18 X. Q. Zou, K. L. Wong, S. Thomas, T. H. Metzger, V. Valtchev and S. Mintova. *Catal. Today*, 2011, 168, 140.
19 A. M. Goossens, B. H. Wouters, V. Buschmann and J. A. Martens. *Adv. Mater.*, 1999,11, 561.
20 J. Q. Zhang, W. B. Fan, Y. Y. Liu and R. F. Li. *Appl. Catal. B*, 2007, 76, 174.
21 X. W. Zhang, Q. Guo, B. Qin, Z. Z. Zhang, F. X. Ling, W. F Sun and R. F. Li. *Catal. Today*, 2010, 149, 212.
22 J. J. Zheng, Q. H. Zeng, Y. M. Yi, Y. Wang, J. H. Ma, B. Qin, X. W. Zhang, W. F. Sun and R. F. Li. *Catal. Today*, 2011, 168, 124.
23 C. He, J. J. Li, P. Li, J. Cheng, Z. P. Hao and Z. P. Xu. *Appl. Catal. B*, 2010, 96, 466.
24 A. Karlsson, M. Sto¨cker and R. Schmidt. *Microporous Mesoporous Mater.*, 1999, 27, 181.
25 A. M. Alsobaai, R. Zakaria and B. H. Hameed. *Fuel Process Technol.*, 2007, 88, 921.
26 B. S. Li, J. Q Xu, X. Li, J. J Liu, S. L. Zuo, Z. Y. Pan and Z. Y. Wu. *Mater. Res. Bull.*, 2012, 47, 1142.
27 J. J. Zheng, X. W. Zhang, Y. Wang, Y. D. Bai, W. F. Sun and R. F. Li. *J. Porous Mater*, 2009, 16,731.
28 B. Xie, H. Y. Zhang, C. G. Yang, S. Y. Liu, L. M. Ren, L. Zhang, X. J. Meng, B. Yilmaz, U. Muller and F. S. Xiao. *Chem. Commun.*, 2011, 47, 3945.
29 U. D. Joshi, P. N. Joshi, S. S. Tamhankar, V. P. Joshi, B. B. Idage, V. V. Joshi and V. P. Shiralkar. *Thermochim. Acta*, 2002, 387, 121.